
Detecting Adversarial Directions in Deep Reinforcement Learning to Make Robust Decisions

Ezgi Korkmaz Jonah Brown-Cohen

Abstract

Learning in MDPs with highly complex state representations is currently possible due to multiple advancements in reinforcement learning algorithm design. However, this incline in complexity, and furthermore the increase in the dimensions of the observation came at the cost of volatility that can be taken advantage of via adversarial attacks (i.e. moving along worst-case directions in the observation space). To solve this policy instability problem we propose a novel method to detect the presence of these non-robust directions via local quadratic approximation of the deep neural policy loss. Our method provides a theoretical basis for the fundamental cut-off between safe observations and adversarial observations. Furthermore, our technique is computationally efficient, and does not depend on the methods used to produce the worst-case directions. We conduct extensive experiments in the Arcade Learning Environment with several different adversarial attack techniques. Most significantly, we demonstrate the effectiveness of our approach even in the setting where non-robust directions are explicitly optimized to circumvent our proposed method.

1. Introduction

Since Mnih et al. (2015) showed that deep neural networks can be used to parameterize reinforcement learning policies, there has been substantial growth in new algorithms and applications for deep reinforcement learning. While this progress has resulted in a variety of new capabilities for reinforcement learning agents, it has at the same time introduced new challenges due to the volatility of deep neural networks under imperceptible adversarial directions originally discovered by Szegedy et al. (2014). In particular, Huang et al. (2017); Kos & Song (2017) showed that the non-robustness

of neural networks to adversarial perturbations extends to the deep reinforcement learning domain, where applications such as autonomous driving, automatic financial trading or healthcare decision making cannot tolerate such a vulnerability.

There has been a significant amount of effort in trying to make deep neural networks robust to adversarial perturbations (Goodfellow et al., 2015; Madry et al., 2018; Pinto et al., 2017). However, in this arms race it has been shown that deep reinforcement learning policies learn adversarial features independent from their worst-case (i.e. adversarial) training techniques (Korkmaz, 2022). More intriguingly, a line of work has focused on showing the inevitability of the existence of adversarial directions, the cost of robust training on generalization, and the intrinsic difficulty of learning robust models (Dohmatob, 2019; Mahloujifar et al., 2019; Korkmaz, 2023; Gourdeau et al., 2019). Given that it may not be possible to make DNNs completely robust to adversarial examples, a natural objective is to instead attempt to detect the presence of adversarial manipulations.

In this paper we propose a novel identification method for directions of volatility in the deep neural policy manifold. Our study is the first one that focuses on detection of adversarial directions in the deep reinforcement learning neural loss landscape. Our approach relies on differences in the curvature of the neural policy in the neighborhood of an adversarial observation when compared to a baseline state observation. At a high level our method is based on the intuition that while baseline states have neighborhoods determined by an optimization procedure intended to learn a policy that works well across all states, each non-robust direction is the output of some local optimization in the neighborhood of one particular state. Our proposed method is computationally efficient, requiring only one gradient computation and two policy evaluations, requires no training that depends on the method used to compute the adversarial direction, and is theoretically well-founded. Hence, our study focuses on identification of non-robust directions and makes the following contributions:

- Our paper is the first to focus on identification of adversarial directions in the deep reinforcement learning policy manifold.

Correspondence to: Ezgi Korkmaz .

Proceedings of the 40th International Conference on Machine Learning, Honolulu, Hawaii, USA. PMLR 202, 2023. Copyright 2023 by the author(s).

- We propose a novel method, Identification of Non-Robust Directions (INRD), to detect adversarial state manipulations based on the local curvature of the neural network policy. INRD is independent of the method used to generate the adversarial direction, computationally efficient, and theoretically justified.
- We conduct experiments in various MDPs from the Arcade Learning Environment that demonstrate the effectiveness of INRD in identifying adversarial directions computed via several state-of-the-art adversarial attack methods.
- Most importantly, we demonstrate that INRD remains effective even against multiple methods for generating non-robust directions specifically designed to evade INRD.

2. Related Work and Background

2.1. Deep Reinforcement Learning

In this paper we focus on discrete action set Markov Decision Processes (MDPs) which are given by a continuous set of states \mathbb{S} , a discrete set of actions \mathbb{A} , a transition probability function $P : \mathbb{S} \times \mathbb{A} \times \mathbb{S} \rightarrow \mathbb{R}$, and a reward function $\mathcal{R} : \mathbb{S} \times \mathbb{A} \times \mathbb{S} \rightarrow \mathbb{R}$. A policy $\pi : \mathbb{S} \rightarrow \mathcal{P}(\mathbb{A})$ assigns a probability distribution on actions $\pi(\cdot|s)$ to each state s . The goal in reinforcement learning is to learn the state-action value function that maximizes expected cumulative discounted rewards $R = \mathbb{E}_{a_t \sim \pi(s_t, \cdot)} \sum_t \gamma^t \mathcal{R}(s_t, a_t, s_{t+1})$ by taking action a in state s . The temporal difference learning is achieved by one step Q-learning which updates $Q(s_t, a_t)$ by

$$Q(s_t, a_t) + \alpha[\mathcal{R}_{t+1} + \gamma \max_a Q(s_{t+1}, a) - Q(s_t, a_t)].$$

2.2. Adversarial Examples

Goodfellow et al. (2015) introduced the fast gradient method (FGM) for producing adversarial examples for image classification. The method is based on taking the gradient of the training cost function $J(x, y)$ with respect to the input image, and bounding the perturbation by ϵ where x is the input image and y is the output label. Later, an iterative version of FGM called I-FGM was proposed by Kurakin et al. (2016). This is also often referred to as Projected Gradient Descent (PGD) as in (Madry et al., 2018) where the I-FGM update is

$$x_{\text{adv}}^{N+1} = \text{clip}_{\epsilon}(x_{\text{adv}}^N + \alpha \text{sign}(\nabla_x J(x_{\text{adv}}^N, y))). \quad (1)$$

where $x_{\text{adv}}^0 = x$. Dong et al. (2018) further modified I-FGM by introducing a momentum term in the update, yielding a method called MI-FGM. Korkmaz (2020) later proposed a

Nesterov-momentum based approach for the deep reinforcement learning domain. The DeepFool method of Moosavi-Dezfooli et al. (2016) is an alternative approach to those based on FGSM. DeepFool performs iterative projection to the closest separating hyperplane between classes. Another alternative approach proposed by Carlini & Wagner (2017a) is based on finding a minimal perturbation that achieves a different target class label. The approach is based on minimizing the loss

$$\min_{s^{\text{adv}} \in \mathbb{S}} c \cdot J(s^{\text{adv}}) + \|s^{\text{adv}} - s\|_2^2 \quad (2)$$

where s is the base input, s_{adv} is the adversarial example, and $J(s)$ is a modified version of the cost function used to train the network. Chen et al. (2018) proposed a variant of the Carlini & Wagner (2017a) formulation that adds an ℓ_1 -regularization term to produce sparser adversarial examples,

$$\min_{s^{\text{adv}} \in \mathbb{S}} c \cdot J(s^{\text{adv}}) + \lambda_1 \|s^{\text{adv}} - s\|_1 + \lambda_2 \|s^{\text{adv}} - s\|_2^2 \quad (3)$$

Our method focusing on identifying non-robust directions in the deep neural policy manifold is the first method to investigate detection of adversarial manipulations in deep reinforcement learning. Our identification method does not require modifying the training of the neural network, does not require any training tailored to the adversarial method used, and uses only two neural network function evaluations and one gradient computation.

2.3. Adversarial Deep Reinforcement Learning

The adversarial problem initially has been investigated by Huang et al. (2017) and Kos & Song (2017) concurrently. In this work the authors show that perturbations computed via FGSM result in extreme performance loss on the learnt policy. Lin et al. (2017) and Sun et al. (2020) focused on timing strategies in the adversarial formulation and utilized the Carlini & Wagner (2017a) method to produce the perturbations. While there is a reasonable body of work focused on finding efficient and effective adversarial perturbations, a substantial body of work focused on building agents robust to these perturbations. While several studies focused on specifically crafted adversarial perturbations, some approached the robustness problem more widely and considered natural directions in a given MDP (Korkmaz, 2023). Pinto et al. (2017) modeled the adversarial interaction as a zero sum game and proposed a joint training strategy to increase robustness in the continuous action space setting. Recently, Gleave et al. (2020) considered an adversary who is allowed to take natural actions in a given environment instead of ℓ_p -norm bounded perturbations and modeled the adversarial relationship as a zero sum Markov game. However, recent concerns have been raised on the robustness of adversarial training methods by Korkmaz (2021; 2022; 2023). In this line of work the authors show that the state-of-the-art adversarial training techniques end up learning similar non-robust

features that allow black-box attacks against adversarially trained policies, and further that adversarial training results in deep reinforcement learning policies with substantially limited generalization capabilities as compared to vanilla training. Thus, with the rising concerns on robustness of recent proposed adversarial training techniques, our work aims to solve the adversarial problem from a different perspective by detecting adversarial directions.

3. Identification of Non-Robust Directions (INRD)

In this section we give the high-level motivation for and formal description of our identification method. We begin by introducing necessary notation and definitions. We denote an original base state by \bar{s} and an adversarially perturbed state by s^{adv} .

Definition 3.1. The *cost of a state*, $J(s, \tau)$, is defined as the cross entropy loss between the policy $\pi(a|s)$ of the agent, and a target distribution on actions $\tau(a)$.

$$J(s, \tau) = - \sum_a \tau(a) \log(\pi(a|s)) \quad (4)$$

Definition 3.2. The *argmax policy*, $\pi^*(a|s)$, is defined as the distribution which puts all probability mass on the highest weight action of $\pi(a|s)$.

$$\pi^*(a|s) = \mathbb{1}_{a=\arg \max_{a'} \pi(a'|s)} \quad (5)$$

We use the following notation for the gradient and Hessian with respect to states s :

$$\begin{aligned} \nabla_s J(s_0, \tau_0) &= \nabla_s J(s, \tau)|_{s=s_0, \tau=\tau_0} \\ \nabla_s^2 J(s_0, \tau_0) &= \nabla_s^2 J(s, \tau)|_{s=s_0, \tau=\tau_0} \end{aligned}$$

3.1. First-Order Identification of Non-Robust Directions (FO-INRD)

As a naive baseline we first describe an identification method based on estimating how much the cost function $J(s, \tau)$ varies under small perturbations. Prior work of (Roth et al., 2019; Hu et al., 2019) has shown that the behavior of deep neural network classifiers under small, random perturbations is different at base versus adversarial examples. Therefore, a natural baseline detection method is: given an input state s_0 sample a small random perturbation $\eta \sim \mathcal{N}(0, \epsilon I)$ and compute,

$$\mathcal{K}(s_0, \eta) = J(s_0 + \eta, \pi^*(\cdot|s_0)) - J(s_0, \pi^*(\cdot|s_0)). \quad (6)$$

The first-order identification method proceeds by first estimating the mean and the variance of \mathcal{K} over a base run (i.e. unperturbed) of the agent in the environment. Next a threshold t is chosen so that a desired false positive rate

(FPR) is achieved (i.e. some desired fraction of the states in the base run lie more than t standard deviations from the mean). Finally, at test time a state encountered by the agent is identified as adversarial if it is at least t standard deviations away from the mean. Otherwise the state is identified as a base observation. As a first attempt, the first-order method can be naturally interpreted as a finite-difference approximation to the magnitude of the gradient at s_0 . If we assume that the first-order Taylor approximation of J is accurate in a ball of radius $r > \epsilon$ centered at s_0 , then

$$\begin{aligned} J(s_0 + \eta, \pi^*(\cdot|s_0)) &\approx J(s_0, \pi^*(\cdot|s_0)) \\ &\quad + \nabla_s J(s_0, \pi^*(\cdot|s_0)) \cdot \eta. \end{aligned}$$

Therefore,

$$\mathcal{K}(s_0, \eta) \approx \nabla_s J(s_0, \pi^*(\cdot|s_0)) \cdot \eta. \quad (7)$$

Thus, for $\eta \sim \mathcal{N}(0, \epsilon I)$ the test statistic $\mathcal{K}(s_0, \eta)$ is approximately distributed as a Gaussian with mean 0 and variance $\epsilon^2 \|\nabla_s J(s_0, \pi^*(\cdot|s_0))\|^2$. Under this interpretation one would expect the test statistics for base and adversarial states to have the same mean with potentially different standard deviations, possibly making it hard to distinguish base from adversarial. However, this is not what we observe empirically, and in fact the first-order method does a decent job of detecting adversarial examples. The method works because, in fact, the mean of $\mathcal{K}(\bar{s}, \eta)$ for base examples \bar{s} is reasonably well separated from the mean of $\mathcal{K}(s^{\text{adv}}, \eta)$ for adversarial examples s^{adv} . The empirical performance of the first-order method thus indicates that the assumption of accuracy for the first-order Taylor approximation of J does not hold in practice. This leads naturally to the consideration of information on the second derivatives (i.e. the local quadratic approximation) of J in order to identify non-robust directions.

3.2. Second-Order Identification of Non-Robust Directions (SO-INRD)

The second-order identification method is based on measuring the local curvature of the cost function $J(s, \tau)$. The method exploits the fact that $J(s, \tau)$ will have larger negative curvature at a base sample as compared to an adversarial sample. In particular, the high level theoretical motivation for this approach is that adversarial samples are the output of a local optimization procedure which attempts to find a nearby perturbed state s^{adv} with a low value for the cost $J(s^{\text{adv}}, \tau)$ for some $\tau \neq \pi^*(\cdot|\bar{s})$. A direction of large negative curvature for $J(s^{\text{adv}}, \tau)$ indicates that a very small perturbation along this direction could dramatically decrease the cost function. Therefore, such points are likely to be unstable for local optimization procedures attempting to minimize the cost function in a small neighborhood. On the other hand, the curvature of $J(s, \tau)$ at a base state \bar{s} is determined by the overall algorithm used to train the deep reinforcement

learning agent. This algorithm optimizes the parameters of the neural network policy while considering all states visited during training, and thus is not likely to be heavily overfit to the state \bar{s} . In particular, we expect larger negative curvature at \bar{s} than at an adversarial state observation s^{adv} . We make the connection between negative curvature and instability for local optimization formal in Section 3.3. Based on the above discussion, a natural choice of metric for distinguishing adversarial versus base samples is the most negative eigenvalue of the Hessian $\lambda_{\min}(\nabla_s^2 J(s_0, \pi^*(\cdot|s_0)))$. While this is the most natural measurement of curvature, it requires computing the eigenvalues of a matrix whose number of entries are quadratic in the input dimension. Since the input is very high-dimensional, and we would like to perform this computation in real-time for every state visited by the agent, computing the value λ_{\min} is computationally prohibitive. Instead we approximate this value by measuring the curvature along a direction which is correlated with the negative eigenvectors of the Hessian. Given this direction, the value that we measure is the accuracy of the first order Taylor approximation of the cost of the given state $J(s, \tau)$. We denote the first order Taylor approximation at the state s_0 in direction η by

$$\tilde{J}(s_0, \eta) = J(s_0, \pi^*(\cdot|s_0)) + \nabla_s J(s_0, \pi^*(\cdot|s_0)) \cdot \eta.$$

The metric we will use to detect adversarial samples is the finite-difference approximation

$$\mathcal{L}(s_0, \eta) = J(s_0 + \eta, \pi^*(\cdot|s_0)) - \tilde{J}(s_0, \eta). \quad (8)$$

To see formally that Equation (8) gives an approximation of the most negative eigenvector of the Hessian, we will assume that the cost function $J(s, \tau)$ is well approximated by its quadratic Taylor approximation at the point s_0 i.e.

$$\begin{aligned} J(s_0 + \eta, \pi^*(\cdot|s_0)) &\approx J(s_0, \pi^*(\cdot|s_0)) \\ &\quad + \nabla_s J(s_0, \pi^*(\cdot|s_0)) \cdot \eta \\ &\quad + \eta^\top \nabla_s^2 J(s_0, \pi^*(\cdot|s_0)) \eta \end{aligned}$$

for sufficiently small perturbation η . Substituting the above formula into Equation (8) yields

$$\mathcal{L}(s_0, \eta) \approx \eta^\top \nabla_s^2 J(s_0, \pi^*(\cdot|s_0)) \eta \quad (9)$$

The above quadratic form is minimized when η lies in the same direction as the most negative eigenvector of the Hessian, in which case

$$\mathcal{L}(s_0, \eta) \approx \lambda_{\min}(\nabla_s^2 J(s_0, \pi^*(\cdot|s_0))) \|\eta\|_2^2 \quad (10)$$

We choose the sign of the gradient direction for measuring the accuracy of the first order Taylor approximation. To motivate this choice note that $-\nabla_s J(s, \tau)$ is locally the direction of steepest decrease for the cost function. If the gradient direction additionally has negative curvature

Algorithm 1 Second Order Identification of Non-Robust Directions (SO-INRD)

Input: The base run mean $\bar{\mathcal{L}}$ and variance $\sigma^2(\mathcal{L})$, identification threshold $t > 0$, parameter $\epsilon > 0$.

for states s_i visited by deep reinforcement learning policy **do**

$$\eta_i = \epsilon \frac{\text{sign}(\nabla_s J(s_i, \pi^*(\cdot|s_i)))}{\|\nabla_s J(s_i, \pi^*(\cdot|s_i))\|_2}$$

$$\tilde{J}(s_i, \eta_i) = J(s_i, \pi^*(\cdot|s_i)) + \nabla_s J(s_i, \pi^*(\cdot|s_i)) \cdot \eta_i$$

$$\mathcal{L}(s_i, \eta_i) = J(s_i + \eta_i, \pi^*(\cdot|s_i)) - \tilde{J}(s_i, \eta_i)$$

if $|\mathcal{L}(s_i, \eta_i) - \bar{\mathcal{L}}| > t \cdot \sigma(\mathcal{L})$ **then**

Identify state s_i as a non-robust state observation

end if

end for

of large magnitude, then small perturbations along this direction will result in even more rapid decrease in the cost function value than predicted by the first-order gradient approximation. Note that this can be true even if the gradient itself has small magnitude, as long as the negative curvature is large enough. Thus, by the discussion at the beginning of Section 3.2, adversarial examples are likely to have relatively smaller magnitude negative curvature in the gradient direction than base examples. Formally, for $\epsilon > 0$ we set

$$\eta(s_0) = \epsilon \frac{\text{sign}(\nabla_s J(s_0, \pi^*(\cdot|s_0)))}{\|\nabla_s J(s_0, \pi^*(\cdot|s_0))\|_2}. \quad (11)$$

To calibrate the detection method we record the mean $\bar{\mathcal{L}} = \mathbb{E}_s[\mathcal{L}(s, \eta(s))]$ and variance $\sigma^2(\mathcal{L}) = \text{Var}_s[\mathcal{L}(s, \eta(s))]$ of our proposed test statistic over states from a base run of the policy in the MDP. Then at test time we set a threshold $t > 0$, and for each state s_i visited by the agent test if

$$|\mathcal{L}(s_i, \eta(s_i)) - \bar{\mathcal{L}}| > t\sigma(\mathcal{L}). \quad (12)$$

If the threshold of t standard deviations is exceeded we identify the state s_i as adversarial, and otherwise identify it as a base state observation. Pseudo-code for the second order method is given in Algorithm 1.

3.3. Negative Curvature and Instability of Local Optimization

In this section we formalize the connection between negative curvature and instability for local optimization procedures that motivated our definition of $\mathcal{L}(s, \eta)$. Given a state s_0 and a target distribution $\tau \neq \pi^*(\cdot|s_0)$, we assume the adversary is trying to find a state s^{adv} minimizing $J(s^{\text{adv}}, \tau)$ among all states close to s_0 by some metric. Formally, let $D_{s_0}(s) \geq 0$ be a convex function of s that should be thought of as measuring distance to s_0 . One standard choice for the distance function is $D_{s_0}(s) = \|s - s_0\|_p^p$. We model the adversary as minimizing the loss

$$f(s) = J(s, \tau) + D_{s_0}(s). \quad (13)$$

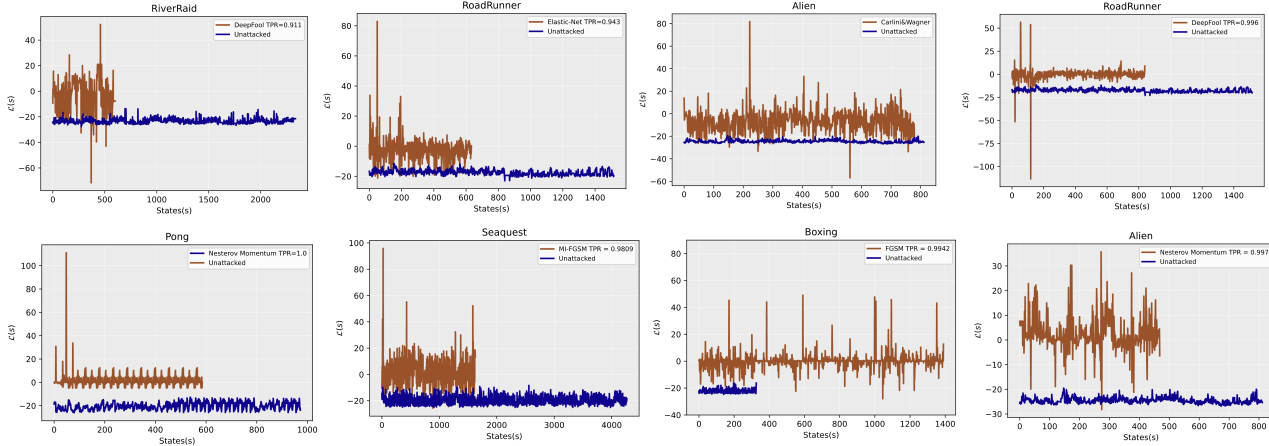


Figure 1. $\mathcal{L}(s)$ for our proposed method SO-INRD vs visited states with corresponding TPR values for the following attack methods: FGSM, MI-FGSM, Nesterov, DeepFool, Carlini&Wagner, Elastic Net Method. TPR values shown in the upper right box of the figure when FPR is equal to 0.01.

In particular, we make the following assumption:

Assumption 3.3. The adversarial state s^{adv} is a local minimum of $f(s)$.

Of course this assumption is violated in practice since different methods used to compute adversarial directions optimize objective functions other than f , and do not necessarily always converge to a local minimum. Nevertheless the assumption allows us to make formal qualitative predictions about the behavior of the second-order identification method that correspond well with empirical results across a broad variety of methods for generating adversarial directions. We now state our main result lower bounding the curvature of $J(s^{\text{adv}}, \tau)$.

Proposition 3.4. For $c > 0$ assume that the maximum eigenvalue of the Hessian $\nabla_s^2 D_{s_0}(s)$ is bounded by c . If s^* is a local minimum of $f(s)$ then $\lambda_{\min}(\nabla_s^2 J(s^*, \tau)) \geq -c$

Proof. Let v be the eigenvector of $\nabla_s^2 J(s^*, \tau)$ corresponding to the minimum eigenvalue. At a local minimum s^* of $f(s)$ the Hessian $\nabla_s^2 f(s^*)$ must be positive semi-definite. Therefore,

$$\begin{aligned} 0 &\leq v^\top \nabla_s^2 f(s^*) v = v^\top \nabla_s^2 J(s^*, \tau) v + v^\top \nabla_s^2 D_{s_0}(s^*) v \\ &\leq \lambda_{\min}(\nabla_s^2 J(s^*, \tau)) + c \end{aligned}$$

Rearranging the above inequality completes the proof. \square

The second order conditions for a local minimum of f imply a lower bound on the smallest eigenvalue of $\nabla_s^2 J(s^*, \tau)$. Thus, by Assumption 3.3, we obtain a lower bound on $\lambda_{\min}(\nabla_s^2 J(s^{\text{adv}}, \tau))$. The assumption that the maximum eigenvalue of the Hessian $\nabla_s^2 D_{s_0}(s)$ is bounded by c is satisfied for example when $D_{s_0}(s) = \frac{c}{2} \|s - s_0\|_2^2$. In contrast, the local curvature of the cost function $J(s, \tau)$ at a base

sample is determined by an optimization procedure that updates the *weights* θ of the neural network policy rather than the states s . If we write $J_\theta(s, \tau)$ to make explicit the dependence on the weights, then the second order conditions for optimizing the original neural network apply to the Hessian with respect to weights $\nabla_\theta^2 J_\theta(s, \tau)$ rather than the Hessian with respect to states $\nabla_s^2 J_\theta(s, \tau)$. Additionally, first order optimality conditions can help to justify the choice of $\nabla_s J(s, \tau)$ as a good direction to check for negative curvature. Indeed by the first order conditions, at a local optimum s^* of $f(s)$ we have

$$0 = \nabla_s f(s^*) = \nabla_s J(s^*, \tau) + \nabla_s D_{s_0}(s^*). \quad (14)$$

Therefore, $\nabla_s J(s^*, \tau) = -\nabla_s D_{s_0}(s^*)$. So assuming the adversary finds a local optimum, $\nabla_s J(s, \tau)$ points in a direction that decreases the distance function $D_{s_0}(s^*)$. Thus sufficiently negative curvature in the direction of $\nabla_s J(s, \tau)$ implies not only that s is not a local minimum of f , but also that the distance function $D_{s_0}(s)$ can be decreased by moving along this direction of negative curvature. To summarize, we have shown that second order optimality conditions arising from computing an adversarial example give rise to lower bounds on the smallest eigenvalue of the Hessian $\lambda_{\min}(\nabla_s^2 J(s, \tau))$. The function $\mathcal{L}(s, \eta)$ used to identify adversarial directions for SO-INRD is a finite difference approximation to

$$\eta^\top \nabla_s^2 J(s, \tau) \eta \geq \lambda_{\min}(\nabla_s^2 J(s, \tau)) \|\eta\|^2.$$

Therefore the results of this section imply that $\mathcal{L}(s, \eta)$ should be larger at adversarial samples than base samples. It is worth noting that the theoretical motivation presented here generalizes straightforwardly to any model which is trained to output a probability distribution given some high-dimensional input (e.g. autoregressive language models). Thus, future research could significantly benefit from further

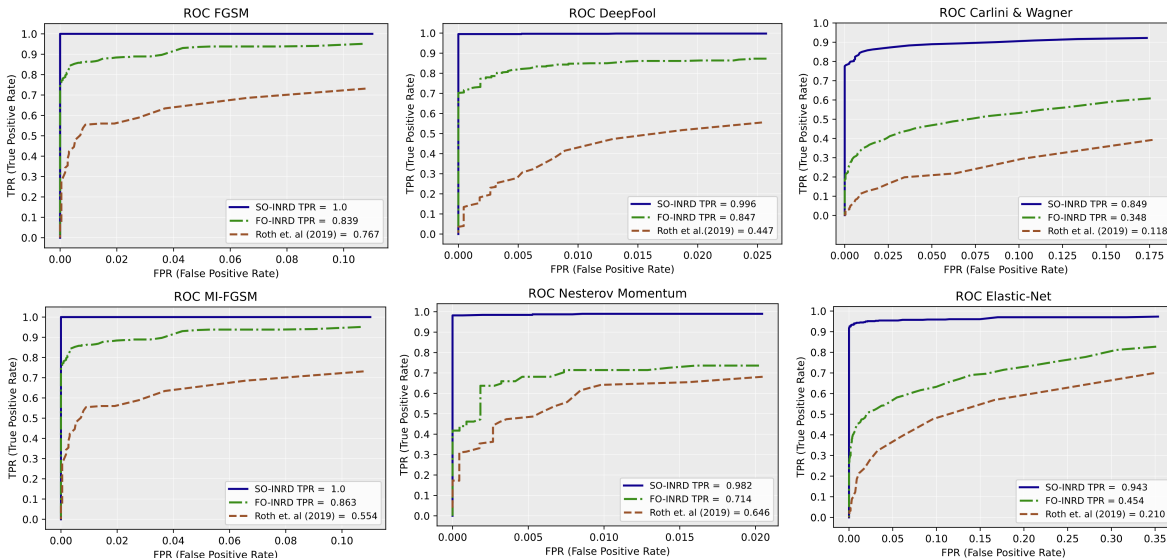


Figure 2. ROC curves of FO-INRD, SO-INRD and OAO method for the following attack methods: FGSM, MI-FGSM, Nesterov Momentum, DeepFool, Carlini&Wagner, Elastic Net Method in RoadRunner. TPR values shown in the lower right box of the figure when FPR is equal to 0.01.

Table 1. True Positive Rates (TPR) for FGSM, MI-FGSM, Nesterov Momentum, Carlini&Wagner, Elastic-Net and DeepFool when False Positive Rate (FPR) is equal to 0.01. The proposed methods SO-INRD and FO-INRD are evaluated, and compared with Roth et al. (OAO) in Riverraid, RoadRunner, Alien, Seaquest, Boxing, Pong, and Robotank games. More results for different FPR values are reported in the supplementary material.

Detection Method-Attack Method	RiverRaid	RoadRunner	Alien	Seaquest	Boxing	Pong	Robotank
SO-INRD FGSM	0.997	1.0	1.0	0.995	0.994	1.0	0.999
FO-INRD FGSM	0.990	0.843	0.803	0.931	0.793	0.622	0.413
OAO FGSM	0.681	0.767	0.885	0.403	0.264	0.424	0.911
SO-INRD M-IFGSM	0.998	1.0	1.0	0.985	0.910	1.0	0.985
FO-INRD M-IFGSM	0.952	0.863	0.991	0.981	0.827	0.622	0.470
OAO M-IFGSM	0.775	0.554	0.929	0.581	0.499	0.679	0.777
SO-INRD Nesterov Momentum	0.995	0.989	0.996	0.952	0.865	1.0	0.954
FO-INRD Nesterov Momentum	0.990	0.714	0.997	0.979	0.746	0.633	0.574
OAO Nesterov Momentum	0.785	0.646	0.925	0.671	0.517	0.687	0.753
SO-INRD Carlini&Wagner	0.910	0.988	0.945	0.723	0.856	0.850	0.713
FO-INRD Carlini&Wagner	0.695	0.594	0.642	0.516	0.785	0.494	0.119
OAO Carlini&Wagner	0.036	0.118	0.018	0.004	0.016	0.028	0.032
SO-INRD Elastic Net	0.777	0.943	0.875	0.687	0.770	0.736	0.815
FO-INRD Elastic Net	0.685	0.454	0.561	0.502	0.743	0.361	0.212
OAO Elastic Net	0.124	0.210	0.060	0.014	0.150	0.092	0.056
SO-INRD DeepFool	0.914	0.996	0.993	0.860	0.951	0.889	0.900
FO-INRD DeepFool	0.841	0.847	0.936	0.777	0.928	0.796	0.268
OAO DeepFool	0.397	0.447	0.611	0.234	0.381	0.367	0.607

utilization of our method in other domains by leveraging the fundamental cut-off between adversarial samples and base samples discovered in our paper.

4. Experiments

In our experiments agents are trained with DDQN (Wang et al., 2016) in the Arcade Learning Environment (ALE)

(Bellemare et al., 2013) from OpenAI (Brockman et al., 2016). For a baseline we compare FO-INRD and SO-INRD with the detection method of OAO proposed by Roth et al. (2019), which is based on estimating the average change in the odds ratio between classes under noise. In Figure 1 we plot the value of $\mathcal{L}(s)$ over states for various games without an adversarial attack and under adversarial attack with the following methods: Carlini & Wagner, Elastic

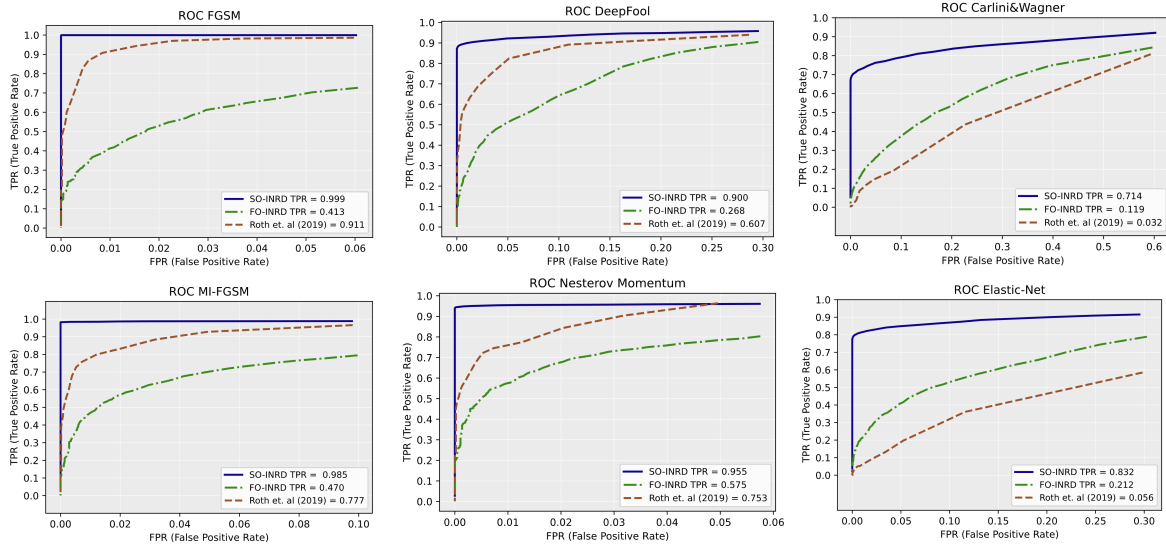


Figure 3. ROC curves of FO-INRD, SO-INRD and OAO method for the following attack methods: FGSM, MI-FGSM, Nesterov Momentum, DeepFool, Carlini&Wagner, Elastic Net Method in Robotank. TPR values are reported in the lower right box of the figure when FPR is equal to 0.01.

Table 2. TPR for Feature Matching for SO-INRD and OAO method FPR=0.01

Feature Matching	Riverraid	RoadRunner	Alien	Sequest	Boxing	Robotank
SO-INRD	0.882	0.863	0.9016	0.955	0.988	0.8978
OAO Method	0.0088	0.006	0.007	0.0146	0.0106	0.0158

Net, Nesterov Momentum, DeepFool, MIFGSM and FGSM. We show in the legends of Figure 1 the true positive rate (TPR) values for the different attacks when false positive rate (FPR) is equal to 0.01. The value of $\mathcal{L}(s)$ for base states is generally well-concentrated and negative. On the other hand, for states computed by the different adversarial attack methods $\mathcal{L}(s)$ is clearly larger, matching the predictions of Proposition 3.4. The fact that $\mathcal{L}(s)$ is consistently larger at adversarial state observations across a wide variety of adversarial perturbation methods indicates that Assumption 3.3 qualitatively captures the behavior of these methods. In particular the FGSM-based methods and DeepFool do not explicitly optimize an objective function of the form $f(s) = J(s, \tau) + D_{s_0}(s)$ as in Assumption 3.3. However, by enforcing a constraint on the distance of the adversarial sample from the original base sample, these methods implicitly solve an optimization problem of the form given in (13), and thus exhibit the qualitative behavior predicted by Proposition 3.4. In Table 1 we show TPR values for FO-INRD, SO-INRD, and the OAO method under the FGSM, MI-FGSM, Nesterov Momentum, DeepFool, Carlini&Wagner, and Elastic-Net attacks when FPR is equal to 0.01. For all of the attack methods in all of the environments SO-INRD is able to detect adversarial perturbations with large TPR. SO-INRD outperforms the other detection methods in all cases except for Nesterov Momentum in Alien and Sequest where FO-INRD has TPR 0.997 and 0.980 while SO-INRD has 0.996 and 0.952. We also observe that while the pertur-

bations computed by FGSM, MI-FGSM, Nesterov Momentum can generally be detected with large TPR values by all the detection methods, the perturbations computed by Carlini&Wagner and the Elastic-Net method are more difficult to detect. Despite the difficulty, SO-INRD achieves TPR values ranging from 0.713 to 0.988 for Carlini&Wagner, and TPR values ranging from 0.687 to 0.943 for Elastic-Net when FPR is equal to 0.01. In Figure 2 and Figure 3 we show ROC curves for each detection method under the FGSM, MI-FGSM, Nesterov Momentum, DeepFool, Carlini&Wagner and Elastic-Net method for RoadRunner and Robotank respectively. In Robotank the OAO method outperforms FO-INRD and even approaches the TPR of SO-INRD for high FPR under FGSM, MI-FGSM, Nesterov Momentum and DeepFool. However for the Carlini&Wagner and Elastic-Net attacks, SO-INRD has a much higher TPR across a wide range of FPR levels.

5. Computing Adversarial Directions Specifically to Evade INRD

Recently, Tramer et al. (2020) introduced a comprehensive methodology for tailoring the optimization procedure used to produce adversarial examples in order to overcome detection and defense methods. In particular, the high level idea is to keep the attack as simple as possible while still accurately targeting the detection method. More specifically,

Table 3. TPR values of INRD in the presence of a identification aware adversary when FPR=0.01.

Detection Method	RiverRaid	RoadRunner	Alien	Seaquest	Boxing	Pong	Robotank
SO-INRD — C&W	0.650	0.849	0.445	0.381	0.710	0.712	0.657
FO-INRD — C&W	0.346	0.348	0.351	0.193	0.621	0.325	0.0973

the methodology is based on designing an attack based on gradient descent on some loss function. Further, minimizing the loss function should correspond closely to subverting the full detection method while still being possible to optimize. Critically, the authors highlight that while the choice of loss function to optimize can be a difficult task, the use of “feature matching” (Gowal et al., 2019) can circumvent most of the current detection methods. We now describe how we applied the methodology discussed above to design detection aware adversaries for SO-INRD. As a first attempt, we tested the “feature matching” approach that was used to break the OAO detection method in Tramer et al. (2020). This approach attempts to match the logits of the adversarial example to those of a base example from a different class in order to evade detection. To optimize the loss for this method we used up to 1000 PGD iterations, and we searched step size varying from 0.01 to 10^{-6} . We find that this method succeeds in reducing the TPR of the OAO method to nearly zero. It is also able to slightly reduce the TPR of our SO-INRD method (see results in Table 2). However, as we will see next, a larger reduction in the TPR of SO-INRD can be achieved by optimizing a modified version of the loss from Carlini & Wagner (2017b). Our next attempt is based on a modification of the Carlini & Wagner (2017b) formulation to additionally minimize the cost function $\mathcal{L}(s)$ used in SO-INRD,

$$\min_{s^{\text{adv}} \in \mathbb{S}} c \cdot J(s^{\text{adv}}) + \|s^{\text{adv}} - s\|_2^2 + \lambda \cdot \mathcal{L}(s^{\text{adv}}). \quad (15)$$

Recall that $\mathcal{L}(s)$ is consistently larger at adversarial examples than at base examples. Thus the above optimization problem attempts to find adversarial examples with as small values of $\mathcal{L}(s)$ as possible. Since the function $\mathcal{L}(s)$ involves taking the sign of the gradient, we use Backwards Pass Differentiable Approximation (BPDA) as introduced in Carlini & Wagner (2017b) to compute the gradients. However, we also tried designing an adversary with a fully differentiable cost function by using a perturbation in the gradient direction (without the sign). We found that this fully differentiable adversary performed significantly worse than the one based on BPDA. We conducted exhaustive grid search over all the parameters in this optimization method: learning rate, iteration number, confidence parameter κ , and objective function parameter λ . In C&W we used up to 30000 iterations to find adversarial examples to bypass detection methods. We searched the confidence parameter from 0 to 50, the learning rate from 0.001 to 0.1, and λ from 0.001 to 10. In our grid search over these hyperparameters we

found that there is a trade-off between the attack success rate and the detection of the perturbations. In other words, if we optimize the perturbation to be undetectable the success rate of the perturbation (i.e. the rate at which the perturbation actually makes the agent choose a non-optimal action) decreases. Therefore, when finalizing the hyperparameters for the SO-INRD detection-aware adversary we restricted our search to a setting where the decrease in the impact of the attack on the policy performance was at most 10%.

Since FO-INRD is based on sampling a random perturbation, we use another approach introduced by Carlini & Wagner (2017b) to minimize the expectation of the original loss function when averaged over the randomness used in the detection method. In particular, we estimate the expectation by computing the empirical mean of the loss over 50 samples from the same noise source. As for the case of SO-INRD we grid search over hyperparameters to achieve as low a TPR as possible while losing at most 10% in the impact of the attack. Table 3 shows the TPR in the adversary-aware setting with the best hyperparameters found for each method. The fact that SO-INRD still performs quite well in the adversary-aware setting is an indication that there is a fundamental trade-off between computing an adversarial direction and minimizing $\mathcal{L}(s)$. This trade-off is further supported by Proposition 3.4, which demonstrates that searching for an adversarial example in a small neighborhood will tend to increase $\mathcal{L}(s)$.

6. Conclusion

In this paper we introduce a novel algorithm INRD, the first method for identification of adversarial directions in the deep neural policy manifold. Our method is theoretically motivated by the fact that local optimization objectives corresponding to the construction of adversarial directions lead naturally to lower bounds on the curvature of the cost function $J(s, \tau)$. We have further shown empirically that the curvature of $J(s, \tau)$ is significantly larger at adversarial states than at base observations, leading to a highly effective method SO-INRD for detecting adversarial directions in deep reinforcement learning. We additionally demonstrate that SO-INRD remains effective in the adversary-aware setting, and connect this fact to our original theoretical motivation. We believe that due to the strong empirical performance and solid theoretical motivation SO-INRD can be an important step towards producing robust deep reinforcement learning policies.

References

- Bellemare, M. G., Naddaf, Y., Veness, J., and Bowling, M. The arcade learning environment: An evaluation platform for general agents. *Journal of Artificial Intelligence Research*, pp. 253–279, 2013.
- Brockman, G., Cheung, V., Pettersson, L., Schneider, J., Schulman, J., Tang, J., and Zaremba, W. Openai gym. *arXiv:1606.01540*, 2016.
- Carlini, N. and Wagner, D. Towards evaluating the robustness of neural networks. In *2017 IEEE Symposium on Security and Privacy (SP)*, pp. 39–57, 2017a.
- Carlini, N. and Wagner, D. A. Adversarial examples are not easily detected: Bypassing ten detection methods. In Thuraisingham, B. M., Biggio, B., Freeman, D. M., Miller, B., and Sinha, A. (eds.), *Proceedings of the 10th ACM Workshop on Artificial Intelligence and Security, AISec@CCS 2017, Dallas, TX, USA, November 3, 2017*, pp. 3–14. ACM, 2017b.
- Chen, P., Sharma, Y., Zhang, H., Yi, J., and Hsieh, C. EAD: elastic-net attacks to deep neural networks via adversarial examples. In McIlraith, S. A. and Weinberger, K. Q. (eds.), *Proceedings of the Thirty-Second AAAI Conference on Artificial Intelligence, (AAAI-18), the 30th Innovative Applications of Artificial Intelligence (IAAI-18), and the 8th AAAI Symposium on Educational Advances in Artificial Intelligence (EAAI-18), New Orleans, Louisiana, USA, February 2-7, 2018*, pp. 10–17. AAAI Press, 2018.
- Dohmatob, E. Generalized no free lunch theorem for adversarial robustness. In Chaudhuri, K. and Salakhutdinov, R. (eds.), *Proceedings of the 36th International Conference on Machine Learning*, volume 97 of *Proceedings of Machine Learning Research*, pp. 1646–1654. PMLR, 09–15 Jun 2019.
- Dong, Y., Liao, F., Pang, T., Su, H., Zhu, J., Hu, X., and Li, J. Boosting adversarial attacks with momentum. In *Proceedings of the IEEE conference on computer vision and pattern recognition*, pp. 9185–9193, 2018.
- Gleave, A., Dennis, M., Wild, C., Neel, K., Levine, S., and Russell, S. Adversarial policies: Attacking deep reinforcement learning. *International Conference on Learning Representations ICLR*, 2020.
- Goodfellow, I., Shelens, J., and Szegedy, C. Explaining and harnessing adversarial examples. *International Conference on Learning Representations*, 2015.
- Gourdeau, P., Kanade, V., Kwiatkowska, M., and Worrell, J. On the hardness of robust classification. In Wallach, H. M., Larochelle, H., Beygelzimer, A., d’Alché-Buc, F., Fox, E. B., and Garnett, R. (eds.), *Advances in Neural Information Processing Systems 32: Annual Conference on Neural Information Processing Systems 2019, NeurIPS 2019, December 8-14, 2019, Vancouver, BC, Canada*, pp. 7444–7453, 2019.
- Gowal, S., Uesato, J., Qin, C., Huang, P.-S., Mann, T. A., and Kohli, P. An alternative surrogate loss for pgd-based adversarial testing. <https://arxiv.org/abs/1910.09338>, 2019.
- Hu, S., Yu, T., Guo, C., Chao, W., and Weinberger, K. Q. A new defense against adversarial images: Turning a weakness into a strength. In Wallach, H. M., Larochelle, H., Beygelzimer, A., d’Alché-Buc, F., Fox, E. B., and Garnett, R. (eds.), *Advances in Neural Information Processing Systems 32: Annual Conference on Neural Information Processing Systems 2019, NeurIPS 2019, December 8-14, 2019, Vancouver, BC, Canada*, pp. 1633–1644, 2019.
- Huang, S., Papernot, N., Goodfellow, Ian an Duan, Y., and Abbeel, P. Adversarial attacks on neural network policies. *Workshop Track of the 5th International Conference on Learning Representations*, 2017.
- Korkmaz, E. Nesterov momentum adversarial perturbations in the deep reinforcement learning domain. *International Conference on Machine Learning, ICML 2020, Inductive Biases, Invariances and Generalization in Reinforcement Learning Workshop.*, 2020.
- Korkmaz, E. Investigating vulnerabilities of deep neural policies. *Conference on Uncertainty in Artificial Intelligence (UAI)*, 2021.
- Korkmaz, E. Deep reinforcement learning policies learn shared adversarial features across mdps. *AAAI Conference on Artificial Intelligence*, 2022.
- Korkmaz, E. Adversarial robust deep reinforcement learning requires redefining robustness. *AAAI Conference on Artificial Intelligence*, 2023.
- Kos, J. and Song, D. Delving into adversarial attacks on deep policies. *International Conference on Learning Representations*, 2017.
- Kurakin, A., Goodfellow, I., and Bengio, S. Adversarial examples in the physical world. *arXiv preprint arXiv:1607.02533*, 2016.
- Lin, Y.-C., Zhang-Wei, H., Liao, Y.-H., Shih, M.-L., Liu, i.-Y., and Sun, M. Tactics of adversarial attack on deep reinforcement learning agents. *Proceedings of the Twenty-Sixth International Joint Conference on Artificial Intelligence*, pp. 3756–3762, 2017.

- Madry, A., Makelov, A., Schmidt, L., Tsipras, D., and Vladu, A. Towards deep learning models resistant to adversarial attacks. In *6th International Conference on Learning Representations, ICLR 2018, Vancouver, BC, Canada, April 30 - May 3, 2018, Conference Track Proceedings*. OpenReview.net, 2018.
- Mahloujifar, S., Zhang, X., Mahmoody, M., and Evans, D. Empirically measuring concentration: Fundamental limits on intrinsic robustness. In Wallach, H. M., Larochelle, H., Beygelzimer, A., d’Alché-Buc, F., Fox, E. B., and Garnett, R. (eds.), *Advances in Neural Information Processing Systems 32: Annual Conference on Neural Information Processing Systems 2019, NeurIPS 2019, December 8-14, 2019, Vancouver, BC, Canada*, pp. 5210–5221, 2019.
- Mnih, V., Kavukcuoglu, K., Silver, D., Rusu, A. A., Veness, J., Bellemare, a. G., Graves, A., Riedmiller, M., Fidjeland, A., Ostrovski, G., Petersen, S., Beattie, C., Sadik, A., Antonoglou, King, H., Kumaran, D., Wierstra, D., Legg, S., and Hassabis, D. Human-level control through deep reinforcement learning. *Nature*, 518:529–533, 2015.
- Moosavi-Dezfooli, S., Fawzi, A., and Frossard, P. Deep-fool: A simple and accurate method to fool deep neural networks. In *2016 IEEE Conference on Computer Vision and Pattern Recognition, CVPR 2016, Las Vegas, NV, USA, June 27-30, 2016*, pp. 2574–2582. IEEE Computer Society, 2016.
- Pinto, L., Davidson, J., Sukthankar, R., and Gupta, A. Robust adversarial reinforcement learning. *International Conference on Learning Representations ICLR*, 2017.
- Roth, K., Kilcher, Y., and Hofmann, T. The odds are odd: A statistical test for detecting adversarial examples. In Chaudhuri, K. and Salakhutdinov, R. (eds.), *Proceedings of the 36th International Conference on Machine Learning, ICML 2019, 9-15 June 2019, Long Beach, California, USA*, volume 97 of *Proceedings of Machine Learning Research*, pp. 5498–5507. PMLR, 2019.
- Sun, J., Zhang, T., Xiaofei, L., Ma, X., Zheng, Y., Chen, K., and Liu, Y. Stealthy and efficient adversarial attacks against deep reinforcement learning. *Association for the Advancement of Artificial Intelligence (AAAI)*, 2020.
- Szegedy, C., Zaremba, W., Sutskever, I., Bruna, J., Erhan, D., Goodfellow, I., and Fergus, R. Intriguing properties of neural networks. In *Proceedings of the International Conference on Learning Representations (ICLR)*, 2014.
- Tramer, F., Carlini, N., Brendel, W., and Madry, A. On adaptive attacks to adversarial example defenses. *NeurIPS*, 2020.
- Wang, Z., Schaul, T., Hessel, M., Van Hasselt, H., Lanctot, M., and De Freitas, N. Dueling network architectures for deep reinforcement learning. *International Conference on Machine Learning ICML.*, pp. 1995–2003, 2016.